



OPEN SHP2 in tumor-associated macrophages prompted the progression of colorectal cancer via modulating STAT3/PI3K signaling induced PD-1-mediated CAR-T cell apoptosis

Jianfa Xu¹, Jingbo Chen², Xiaoyu Zhang¹, Zibo Zhang¹ & Guiying Wang³✉

To investigate the effect of tumor-associated macrophage tyrosine phosphatase on the progression of colorectal cancer (CRC) and its mechanism. Bioinformatics analysis was used to analyse genes specifically expressed in CRC; The SW480 cell line of CRC and THP-1 macrophages were co-cultured. The effect of SHP2 on CRC was tested by tumor-bearing nude mice model. The relative expression levels of p-SHP2, p-STAT3, p-PI3K, p-Src, MMP2, MMP9, Cyclin D1, CD9, TSG101, CD63, PD-L1, Cyclin A and PCNA in THP-1 cells were detected by Western blot. Cell migration assay and Transwell migration and invasion assay were performed to examine the migration and invasion ability of SW480 cells, and monoclonal proliferation assay was used to detect the proliferation ability of SW480 cells. A co-culture system of CRC cell line SW480, macrophages THP-1 and CAR-T cells was constructed, and the expression of Bax, Caspase-3 and Caspase-9 in CAR-T cells was detected by Western blot. In addition, the relative fluorescence intensity of Bax in CAR-T cells was detected by immunofluorescence staining. Bioinformatics analysis found that SHP2 is highly expressed specifically in CRC; Specific overexpression of SHP2 in THP-1 cells could promote the expression of p-STAT3, p-PI3K, p-Src, MMP2, MMP9, Cyclin D1, Cyclin A and PCNA as well as the expression of CD9, TSG101, CD63 and PD-L1 in exosomes, and promote the proliferation, migration and invasion ability of SW480 cells. In addition, SHP2 can promote the expression of Bax, Caspase-3 and Caspase-9 in CAR-T cells. Activation of TAM-intrinsic SHP2 is significantly associated with upregulation of STAT3/PI3K signaling and PD-1-related CAR-T cell apoptosis, suggesting that it participates in shaping the immunosuppressive microenvironment of CRC and promoting disease progression. This study provides strong rationale for leveraging macrophage SHP2 as an entry point to optimize immunotherapy.

Keywords Colorectal cancer, Tumor-associated macrophages, CAR-T cells, SHP2, STAT3/PI3K signalling pathway

Colorectal cancer (CRC) has become the most common malignant tumour in the digestive system, and according to the latest global cancer statistics, the number of new cases per year is more than 1.9 million, which is about one-tenth of the total number of new cases of cancer and ranks third; and it leads to 935,000 deaths per year, which, as the second largest killer of cancer-related deaths, creates a huge burden of disease globally¹. Meanwhile, according to the latest national cancer statistics published by the National Cancer Centre of China in 2022, the new incidence rate of colorectal cancer ranked the second in the total number of cases after lung cancer. Nowadays, with the improvement of medical technology, endoscopic resection or surgical resection of early stage colorectal cancer has a good therapeutic effect, with a 5-year survival rate of more than 90%. Unfortunately,

¹Department of Orthopaedics, The Fourth Hospital of Hebei Medical University, Shijiazhuang 050011, China.

²Department of Pharmacy, Shijiazhuang People's Hospital, Shijiazhuang 050026, China. ³Department of Gastrointestinal Surgery, The Second Hospital of Hebei Medical University, 215 West Heping Road, Shijiazhuang City 050061, China. ✉email: wangguiying@hebm.edu.cn

however, due to the insidious onset of colorectal cancer, patients are already in the middle to late stage when they seek medical treatment, and about 20% of patients are accompanied by metastasis². Despite advances in surgery and multimodal therapy, outcomes for patients diagnosed at advanced stages remain unsatisfactory, highlighting the need to better understand tumor-immune interactions that drive disease progression and therapeutic resistance.

The tumor microenvironment (TME) critically shapes antitumor immunity. Among its cellular constituents, tumor-associated macrophages (TAMs) promote angiogenesis, matrix remodeling, immune suppression, and metastatic dissemination³. Mechanistically, TAMs secrete matrix metalloproteinases and immunosuppressive cytokines (e.g., IL-10, TGF- β) and can express PD-L1, thereby dampening T-cell activation^{1,4}. T cells, as the main participants in cellular immunity, are considered to be the effector cells of CARs, which can be genetically modified to express CARs. Chimeric antigen receptor (CAR)-T cells have transformed outcomes in hematologic malignancies but face formidable barriers in solid tumors, where hypoxia, acidosis, and suppressive myeloid populations curb CAR-T trafficking and effector function^{5–8}. In particular, PD-1/PD-L1 signaling within the TME contributes to CAR-T dysfunction and apoptosis.

Src-homology-2-containing protein tyrosine phosphatase 2 (SHP2, encoded by PTPN11) is a central signal integrator downstream of receptor tyrosine kinases and adaptor proteins (e.g., EGFR, GAB1). Upon activation, SHP2 modulates multiple pathways—including ERK/MAPK, PI3K-AKT, Rho GTPases, NF- κ B/NFAT, and STATs—that govern macrophage phenotype and function. Emerging evidence implicates SHP2 in regulating TAM-driven tumor progression and immune suppression^{9–11}; however, how TAM-intrinsic SHP2 influences CRC progression and the fate of CAR-T cells within the CRC microenvironment remains insufficiently defined.

Here, we hypothesize that SHP2 in TAMs promotes CRC progression by activating STAT3/PI3K signaling, which enhances exosomal output and PD-L1-related immunosuppression, thereby inducing PD-1-mediated apoptosis of CAR-T cells. To test this, we integrate bioinformatics analyses with co-culture systems (THP-1 macrophages, SW480 CRC cells, and CAR-T cells) and *in vivo* tumor models to define the SHP2-STAT3/PI3K axis in TAMs and its impact on CRC cell proliferation, migration/invasion, exosome secretion, and CAR-T survival. This study aims to clarify a macrophage-centered mechanism that links SHP2 signaling to CAR-T vulnerability in CRC and to nominate macrophage SHP2 as a potential target to improve immunotherapy efficacy.

Methods

Bioinformatics analysis

The GSE28000 colorectal cancer dataset was selected from the GEO database and was subjected to differential gene analysis by the DESeq2 package and visualised by the ggplot2 package to draw volcano plots ($\log_2FC > 1$, $p < 0.05$). KEGG enrichment analysis of genes was performed by clusterProfiler package in R language. We selected colorectal cancer dataset from GEPIA database (<http://gepia.cancer-pku.cn/>) and analysed the co-expression relationship between SHP2 and Src, Src and STAT3, Src and PI3K, PI3K and MMP9, PI3K and cyclin A2 by Spearman analysis and visualisation. correlation scatter plots were obtained. A protein-protein interaction (PPI) network based on gene overlap was constructed using STRING, and the interactions were visualised using the MCC algorithm in the CytoHubba plug-in of the Cytoscape software to obtain the top 5 hub genes in the PPI network.

Cell culture

SW480 cells, THP-1 cells and CAR-T cells were purchased from Hebei Senlang Biotechnology Co., Ltd. Complete media containing 90% RPMI-1640 medium (Gibco, C22400500BT), 10% fetal bovine serum (FBS), and 1% penicillin purchased from the National Biomedical Cell Line Resource Center (BMCR) was cultured at 37 °C in a 5% CO₂ incubator with saturated humidity and streptomycin mixture. Cells were passaged every 2–3 days. Cells in logarithmic growth phase on the 3rd and 5th day were then collected.

Construction of the SHP2 overexpression vector

The coding sequence (CDS) region of SHP2 was obtained from the NCBI database by searching for its transcript number. The pSIH1-H1-copGFP-T2A-Puro vector serves as a backbone to specifically overexpress the SHP2 gene in mice via the GPP Web Portal. The synthesized Lentivirus were annealed and cloned into the pLKO_005 vector. This construct was then introduced into the pHAGE-CD19 vector equipped with a macrophage-specific synthetic promoter through PCR, enzyme digestion, and T4 ligase linking. The pHAGE-CD19, psPAX2, and pMD2.G plasmids were co-transfected into 293 T cells using Lipo8000. The medium was changed to DMEM containing 10% FBS the next day. After 72 h, the supernatant was collected, and centrifuged at 3000 rpm for 15 min at 4 °C, and the viral fluid was stored at –80 °C.

Co-culture system

THP-1 cells were inoculated into a cell culture plate. A permeable polycarbonate membrane was placed on the bottom lay of the Transwell chamber, and the SW480 cells was cultured in the Transwell chamber. Then, the Transwell chamber was put into the culture plate to construct a co-culture system of SW480 cells and THP-1. Meanwhile, CAR-T cells were seeded into the culture plate, so SW480 cells and THP-1 cells were co-cultured in Transwell chamber, and PD-1 monoclonal antibody was added. The cells were divided into NC group, SHP2-OE group, co-culture + NC group and co-culture + SHP2-OE group.

Tumor-bearing nude mice model

Twenty-four 6-week-old BALB/c male nude mice (18 ± 1 g) were purchased from Henan SCBS Biotechnology Co., Ltd. Mice are fed in an SPF environment of 18–25 °C for 1 week. The co-cultured SW480 cells and THP-1

cells were inoculated with a volume of $1 \times 10^7/200\mu\text{l}$ /nude mouse. Mice are weighed, numbered by body weight and cage order, and animals are randomly assigned. Divided into 4 groups of 6 animals. During inoculation, the needle was inserted from the slightly upper part of the waist of the nude mouse side. The distance from the inoculation point was less than the length of the needle. The needle should pass through the head, and the skin or muscle layer was not be punctured. Moreover, the inoculation was completed within 1h. Tumors were measured the next day after the tumor was formed successfully. Then, tumor volume was calculated. Tumor implantation was performed under inhaled isoflurane anesthesia (induction ~ 3–4%, maintenance ~ 1.5–2%) with pre-emptive and postoperative analgesia. Procedures were conducted aseptically; animals were placed on a warming pad until full recovery and monitored at least once daily for general condition, body weight, and wound healing. Humane endpoints included > 15–20% body-weight loss, ulceration/necrosis, impaired mobility or self-care, or tumor burden exceeding, for example, any single diameter > 1.5 cm or ~ 1,500 mm³. Animals meeting endpoints were euthanized in accordance with institutional and AVMA guidelines (e.g., CO₂ asphyxiation followed by a secondary physical method/cervical dislocation). All in vivo procedures were approved by the Animal Ethics Committee of The Fourth Hospital of Hebei Medical University (Approval No.: 2023124) and conducted in accordance with institutional guidelines and the ARRIVE recommendations.

Isolation of exosomes

To generate exosome-free media, exosomes present in fetal bovine serum (Thermo Fisher Scientific, A5256701) were centrifuged overnight at 10,000 g and then filtered through a 0.2 μm syringe mounted filter (Millipore, Burlington, MA). This exosome depleted fetal bovine serum was used for cell culture (DMEM supplemented with 10% exosome free fetal bovine serum). To isolate exosomes, cell supernatants were collected and centrifuged at 2000 \times g and 10,000 \times g for 30 min at 4°C, respectively. The final supernatant was filtered through a 0.22 μm syringe filter (Millipore Burlington, MA) and ultracentrifuged at 120000 \times g for 70 min. Afterwards, the spheroidized vesicles were washed with phosphate buffered saline (PBS) and centrifuged again at 120000 \times g for 70 min. Exosomal markers were determined by Western blot.

Cell migration assay

Parallel lines were drawn on the floor of the 6-well plate using markers. After digestion of SW480 cells, a cell suspension was prepared with trypsin and plated at a concentration of 5×10^5 cells/mL. The next day, the entire cell layer was scratched with 1mL sterile pipette tips, spaced 4 mm vertically apart, perpendicular to the marking line. After washed with PBS, the serum-free medium was placed in a constant temperature incubator containing 95% O₂ and 5% carbon dioxide at 37°C, and photographed at 0 h and 48 h, respectively. The width of the scratch was calculated using Image-Pro Plus software.

Transwell

A transpore chamber with a 24-well, 8.0 μm pore membrane was used. 1×10^5 SW480 cells per well were seeded in 100 μL of serum-free medium, and 600 μL of complete medium was added to the lower chamber as chemotactic agent. After incubation at 37 °C for 24 h, the remaining cells on the upper surface of the membrane were removed with a cotton swab, and the cells on the lower surface of the membrane were migrating cells. After fixation with 4% paraformaldehyde and staining with 0.1% crystal violet solution, the cells were photographed through a filter using an inverted fluorescence microscope. In addition to 100 μL of 1: 8 DMEM diluted matrigel for 6 h, the cells were incubated for 48 h, then were seeded on the membrane for the above trans-pore invasion experiment.

Monoclonal proliferation assay

SW480 cells were collected, trypsinized, counted, and incubated in an incubator at 37 °C for approximately 2 weeks until visible cell colonies were present. The medium was then discarded and the cells were washed three times with PBS, fixed with methanol for 15 min, air-dried and stained with crystal violet for 30 min. Lastly, the cells were scanned and photographed, and visible cell colonies were counted.

Immunofluorescence staining

Cleaned the slides with anhydrous ethanol and distilled water, and dried thoroughly or in an oven. Soaked the slides in 70% ethanol for at least 30 min and dried in a sterile environment. Collected the cells in a cell culture and obtained a cell sediment by centrifugation. Resuspended in a suitable volume of culture medium. Used a pipette to add an appropriate amount of cell suspension to the center of the slide. The cell concentration was adjusted according to the experimental requirements. Placed the slide with the cells in an incubator, usually at 37 °C, 5% CO₂, and incubated for a certain period of time until the cells adhered to the surface of the slide. Gently washed off the unattached cells and medium residues with PBS buffer, usually 3 times for 5 min each. Placed the slide in a fixing solution to fix the cells, usually for 15 min. Rinsed the slides again with PBS to remove the fixative. Selected the appropriate stain according to the needs of the experiment, stained for a certain period of time, and then rinsed with PBS. Added an appropriate amount of sealing agent dropwise to the slide with cells, and carefully covered the slide with a coverslip to avoid creating air bubbles. Placed the slide in a cool place to dry and prepared for further experiments.

Cells were fixed with 4% paraformaldehyde at room temperature for 10 min and washed three times with PBS. Membranes were permeabilized with 1% Triton X-100 for 10 min and washed three times with PBS. Primary antibodies were added and incubated overnight at 4 °C. After three PBS washes, secondary fluorescent antibodies were added and incubated in the dark at room temperature for 1.5 h, followed by three PBS washes. Cells were then mounted with DAPI-containing mounting medium and observed and photographed under a fluorescence microscope.

Western blot

THP-1 cells and CAR-T cells in the two co-culture systems were lysed and centrifuged at 4 °C to extract proteins. SDS-PAGE gel was prepared, and protein sample was added to the wells. Then, SDS-PAGE gel electrophoresis was performed. Afterwards, the protein was transferred to PVDF membrane, blocked with 5% skim milk powder. Primary antibodies p-SHP2, p-STAT3, p-PI3K, p-Src, MMP2, MMP9, Cyclin D1, Cyclin A, PCNA, Bax, Caspase-3, Caspase-9 and GAPDH were added, washed with TBST for 3 times, placed in the secondary antibody solution, shaken and incubated for 2 h, then washed with TBST for 3 times, exposed and developed. The protein bands were analyzed with ECL method.

Statistical analysis

All statistical analysis were implemented with SPSS22.0 software and Graphpad Prism Software 9.0. If the experimental data meets the requirements, the data will be deleted. The data was expressed as (mean ± SEM). t-test was used for the comparisons between groups. The experiment was repeated at least three times in each group, and $P < 0.05$ was regarded as statistically significant.

Ethical approval

All in vivo procedures were reviewed and approved by the Animal Ethics Committee of the Fourth Hospital of Hebei Medical University (Approval No. 2023124), and were conducted in strict accordance with institutional guidelines and the ARRIVE recommendations. The animal facility is licensed by the Laboratory Animal Center of the Fourth Hospital of Hebei Medical University under SYXK (Ji) 2022-011. Randomization and blinding were implemented where feasible; humane endpoints and monitoring schedules were predefined, and anesthesia/analgesia were used to minimize pain and distress. Conflicts of Interest.

Results

Bioinformatics analysis results

We passed the volcano plot (Fig. 1 A) to see the statistical significance of gene expression differences, and the KEGG enrichment analysis data were used to demonstrate the enrichment results in bubble plots (Fig. 1B), i.e., to show the differential expression of the pathways involved in the enrichment. Selecting CRC samples through GEPIA database, we found that SHP2 and Src were positively correlated (p -value = 4.6×10^{-10} ; $R = 0.4$) (Fig. 1C); Src and STAT3 were positively correlated (p -value = 3.1×10^{-9} ; $R = 0.52$) (Fig. 1D); Src and PI3K were positively correlated (p -value = 5.7×10^{-12} ; $R = 0.59$) (Fig. 1E); PI3K and MMP9 were positively correlated (p -value = 0.0016; $R = 0.3$) (Fig. 1F); PI3K and cyclin A2 were positively correlated (p -value = 2.5×10^{-9} ; $R = 0.42$) (Fig. 1G); STAT3 and PD-1 were positively correlated (p -value = 6.5×10^{-13} ; $R = 0.49$) (Fig. 1H). Hub target proteins were identified by PPI networks (Fig. 1I), and PPI networks were obtained from the STRING database using the CytoHubba plugin of Cytoscape software for the top five hub genes, including ERBB2, PIK3R1, EGF, AKT1, KRAS (Fig. 1J).

SHP2 in TAMs promotes colorectal cancer development

First, the effect of SHP2 in TAM on the development of CRC was examined by the tumor-bearing nude mice model, showing that there was no significant difference in tumor volume between the NC group and the SHP2-OE group. After co-culture of THP-1 cells and SW480 cells, tumor volume was significantly increased in SHP2-OE group compared with NC group (Fig. 2). The above results suggest that SHP2 in TAMs can promote CRC progression.

SHP2 could promote the expression of TAM cyclin and the proliferation of SW480 cells in CRC

Western blot showed that the relative protein expression levels of Cyclin D1, Cyclin A and PCNA were not significantly different between NC group and SHP2-OE group. After co-culture of THP-1 cells and SW480 cells, the relative protein expression of them in SHP2-OE group was significantly higher than that in NC group. There was no significant difference in the number of clones between NC group and SHP2-OE group based on the monoclonal proliferation assay. After co-culture of THP-1 cells and SW480 cells, the number of clones in SHP2-OE group was significantly higher than that in NC group, which indicated that SHP2 can promote the expression of cyclin of TAM and the proliferation of SW480 cells in CRC (Fig. 3).

SHP2 can promote the activation of STAT3/PI3K signaling pathway of TAMs and the production of exosomes in CRC

Western blot showed that the relative protein expression levels of p-STAT3, p-PI3K and p-Src in SHP2-OE group were slightly lower than those in NC group. After co-culture of THP-1 cells and SW480 cells, the relative protein expression of p-SHP2 in SHP2-OE group was significantly lower than that in NC group, and the relative protein expression of p-STAT3, p-PI3K and p-Src increased significantly. Western blot analysis showed that the expression levels of CD9, TSG101, CD63 and PD-L1 were not significantly different between NC group and SHP2-OE group. However, the relative protein expression of p-STAT3, p-PI3K, p-Src, CD9, TSG101, CD63, and s-PD-L1 was significantly increased in the SHP2-OE group compared with the NC group after co-culture of THP-1 cells with SW480 cells (Fig. 4). It suggested that SHP2 can promote the activation of STAT3/PI3K signaling pathway of TAM and the production of exosomes in CRC.

SHP2 could promote the expression of MMPs of TAM in CRC and the migration and proliferation of SW480 cells

The results of Western blot showed that the relative protein expression levels of MMP-2 and MMP-9 in SHP2-OE group were not significantly different from those in NC group. After co-culture of THP-1 cells and SW480 cells, the relative protein expression of MMP-2 and MMP-9 in SHP2-OE group was significantly higher than that in

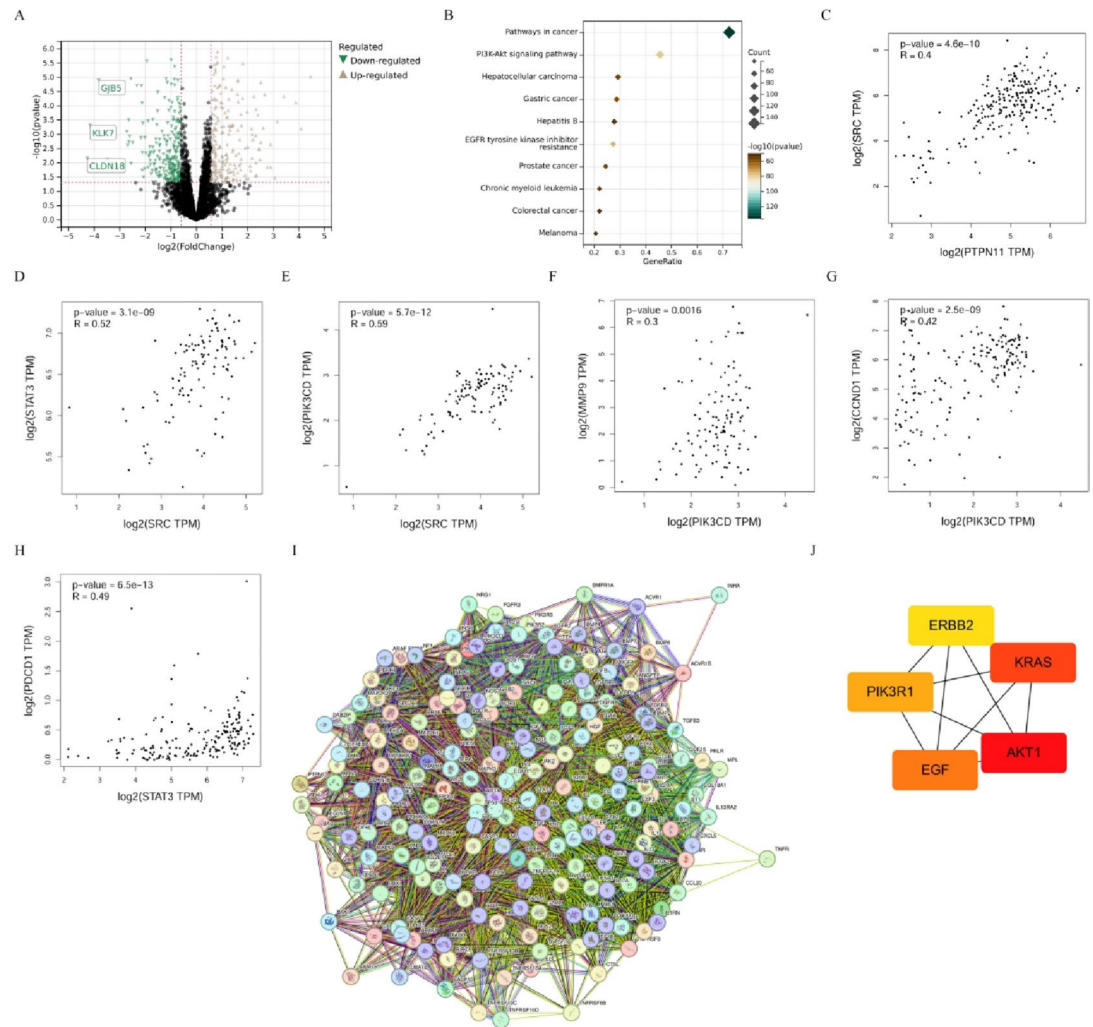


Fig. 1. Bioinformatics analyses. A, Volcano plot of differentially expressed genes generated with the DESeq2 package in R. B, KEGG pathway enrichment dot plot generated with clusterProfiler (R). Pathway annotations were obtained from the KEGG database (Kyoto Encyclopedia of Genes and Genomes, Kanehisa Laboratories) and cited according to the official guidelines; no KEGG pathway images were reproduced^{12,13}. C–H, Pairwise co-expression correlations in colorectal cancer datasets from GEPIA: C, PTPN11 (SHP2) vs. SRC; D, SRC vs. STAT3; E, SRC vs. PI3K; F, PI3K vs. MMP9; G, PI3K vs. CCNA2 (Cyclin A2); H, STAT3 vs. PDCD1 (PD-1). I, Protein–protein interaction (PPI) network of differentially expressed genes constructed using the STRING database. J, Top five hub genes identified with cytoHubba in Cytoscape.

NC group. Cell migration assay showed that there was no significant difference in cell healing rate between NC group and SHP2-OE group. After co-culture of THP-1 cells and SW480 cells, compared with NC group, the healing rate of SHP2-OE group was significantly higher. Transwell assay showed that there was no significant difference in the number of migrating and invading cells between NC group and SHP2-OE group. Identically, the number of migrating and invading cells in SHP2-OE group was significantly higher than that in NC group after co-culture of THP-1 cells and SW480 cells (Fig. 5). It has proved that SHP2 can promote the expression of MMPs of TAM in CRC and the migration and invasion of SW480 cells.

SHP2 in TAM accelerates CAR-T cell apoptosis by promoting exosome secretion

A co-culture system of THP-1 cells, SW480 cells and CAR-T cells was constructed and treated with PD-1 monoclonal antibody. CAR-T cells were then detected using Western blot and Immunofluorescence staining. The results of Western blot showed that the relative protein expression of Bax, Caspase-3 and Caspase-9 had no significant difference between NC group and SHP2-OE group. After co-culture, the relative protein expression of Bax, Caspase-3 and Caspase-9 in the SHP2-OE group was significantly higher than that in the NC group. However, the relative protein expression of Bax, Caspase-3 and Caspase-9 in the NC and SHP2-OE groups was significantly reduced and the significant difference was eliminated by the continued addition of PD-1 monoclonal antibody. Immunofluorescence staining showed that there was no significant difference in the relative fluorescence intensity of Bax between the NC group and the SHP2-OE group. After co-culture, the

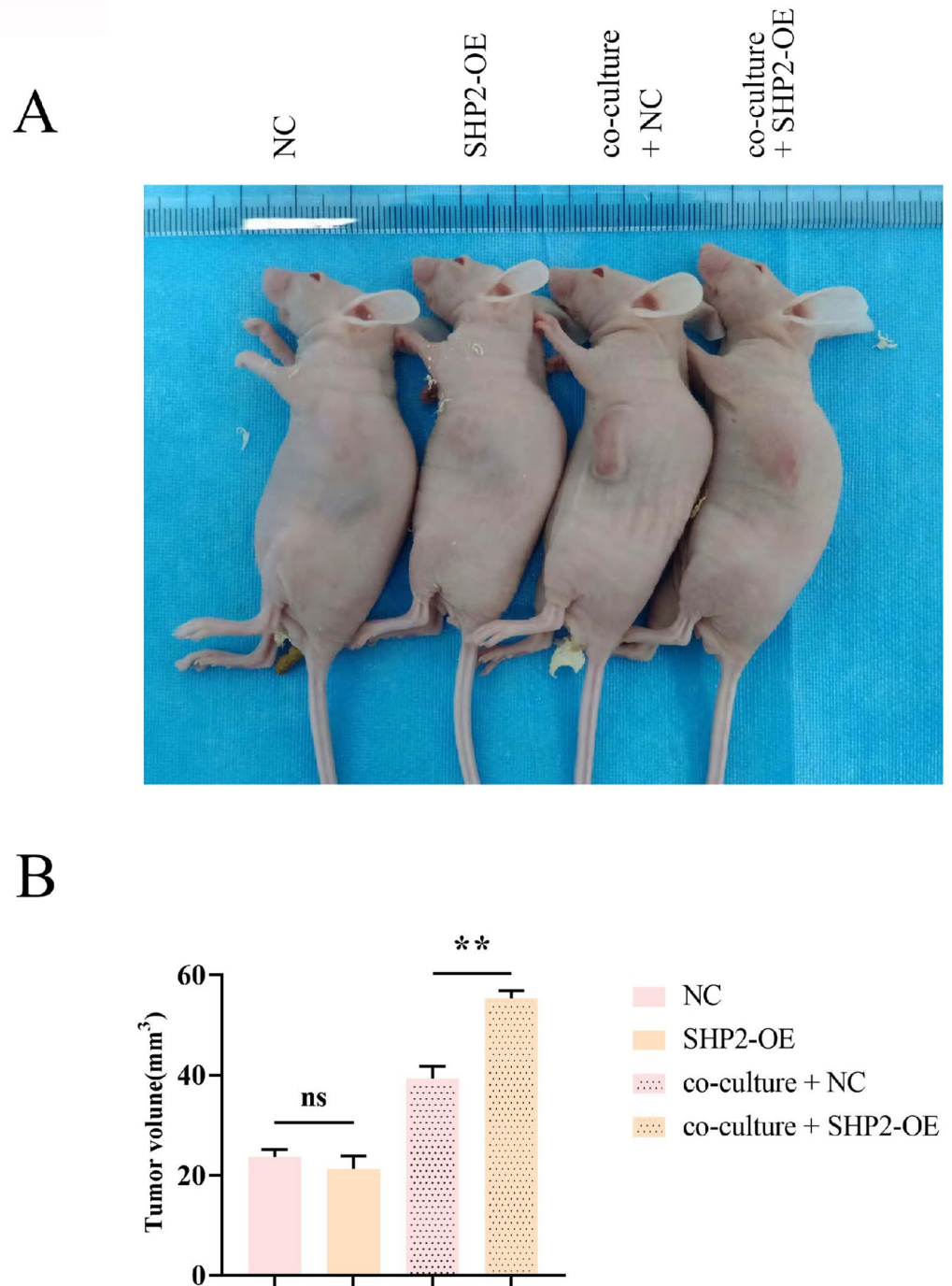


Fig. 2. Impact of SHP2 in tumour-associated macrophages on CRC progression. A: Graph showing the results of subcutaneous transplantation tumour experiments in nude mice; B: Statistical histogram of tumour volume in subcutaneous graft tumour experiments in nude mice; There was no significant difference in tumour volume between the NC and SHP2-OE groups. The tumour volume in the co-culture + SHP2-OE group was significantly larger than that in the co-culture + NC group. Data are expressed as mean \pm SD. ^{ns} $P > 0.05$; ^{**} $P < 0.01$.

relative fluorescence intensity of Bax in the SHP2-OE group was significantly higher than that in the NC group. After the addition of PD-1 monoclonal antibody, the relative fluorescence intensity of Bax in the NC group and SHP2-OE group was significantly reduced and the difference was not significant, indicating that SHP2 in TAM promotes the secretion of exosomes, thereby promoting the apoptosis of CAR-T cells (Fig. 6). Activation of TAM-intrinsic SHP2 is significantly associated with upregulation of STAT3/PI3K signaling and PD-1-related CAR-T cell apoptosis, suggesting that it participates in shaping the immunosuppressive microenvironment of CRC and promoting disease progression (Fig. 7).

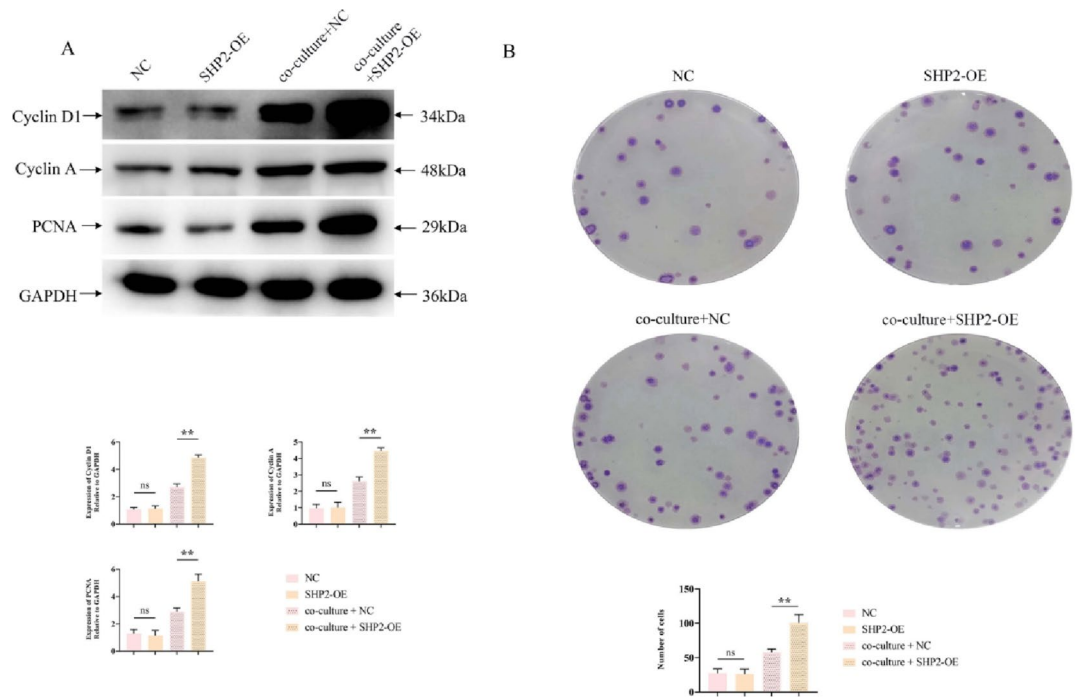


Fig. 3. Effects of SHP2 on CRC cell proliferation. **A** Western blot in THP-1–derived TAMs (all bands from THP-1/TAMs; SW480 was used only to establish co-culture conditions) for Cyclin D1, Cyclin A, and PCNA. Bar graphs show GAPDH-normalized relative protein levels ($n = 3$, mean \pm SD). **B:** SW480 colony formation (monoclonal proliferation) assay under the indicated co-culture conditions and quantification of colony numbers. SHP2 overexpression in TAMs increases cell-cycle protein levels in TAMs and promotes CRC cell proliferation. ns, $P > 0.05$; **, $P < 0.01$.

Discussion

CRC is the second leading cause of cancer-related deaths worldwide, and more than 90% of all colorectal cancer cases are adenocarcinomas arising from glandular epithelial cells of the colon and/or rectum, which occur when these epithelial cells acquire epigenetic or genetic mutations that allow them to replicate and survive excessively^{14,15}. CRC has become a worldwide concern due to its severe metastasis and recurrence. Approximately one-third of patients have metastatic disease at the time of their first diagnosis. Surgery, chemotherapy and radiotherapy remain the main treatment strategies for CRC. However, some early-stage patients eventually relapse after surgical resection, and the survival rate of late-stage patients is extremely low, suggesting an urgent need for new therapeutic strategies, and it is at this time that immunotherapy is beginning to be widely discussed¹⁶.

We focused on the SHP2–STAT3/PI3K axis for the following reasons. As a downstream signaling integrator of multiple receptor tyrosine kinases (e.g., EGFR) and adaptor proteins (e.g., GAB1), SHP2 can concomitantly regulate the ERK/MAPK, PI3K–AKT, and STAT pathways—cascades that are central to myeloid cell phenotypes and immunosuppression. Prior studies indicate that SHP2 activation is associated with elevated IL-10, TGF- β , and PD-L1 expression, increased exosomal cargo loading, and extracellular matrix remodeling¹⁷. In the context of colorectal cancer, this signaling axis provides a biologically plausible link to tumor progression and CAR-T dysfunction, aligning with the molecular and functional readouts observed in our study.

Macrophages, as an essential innate immune cells for maintaining homeostasis in vivo and resisting foreign pathogens, exhibit high plasticity and perform a variety of supporting functions that specifically target different tissue compartments. As a result, abnormal macrophage function has contributed to the development of several diseases, including cancer, fibrosis, and diabetes. In the context of cancer, tumor-associated macrophages (TAMs) in the tumor microenvironment (TME) generally promote cancer cell proliferation, immunosuppression, and angiogenesis to support tumor growth and metastasis. In general, the abundance of TAMs in tumors is associated with poor disease prognosis. Therefore, the development of cancer immunotherapy based on TAMs has aroused great concern^{18,19}. As an important player in growth factor and cytokine signaling, SHP2 is frequently upregulated or mutated in tumors, which usually contributes to the growth of cancer. Structurally, there are two SH2 domains, a protein tyrosine phosphatase (PTP) domain and a c-terminal tail containing phosphorylated tyrosine residues. SHP2 enhances Src activity by removing phosphorylation of certain negative regulatory sites of Src^{20,21}. It also promotes PI3K–AKT or RHO activation, reduces STAT5 phosphorylation, increases STAT3 phosphorylation and may affect NF- κ B or NFAT pathways, making it difficult to determine the function of SHP2^{22,23}. However, STAT3/PI3K signaling pathway can regulate cell proliferation and exosome secretion. And SHP2 also has a great influence on cell proliferation as well as migration ability. Cyclin D1, Cyclin A and PCNA each play different roles in the cell cycle, regulating the progression of cells from one phase to another. They work

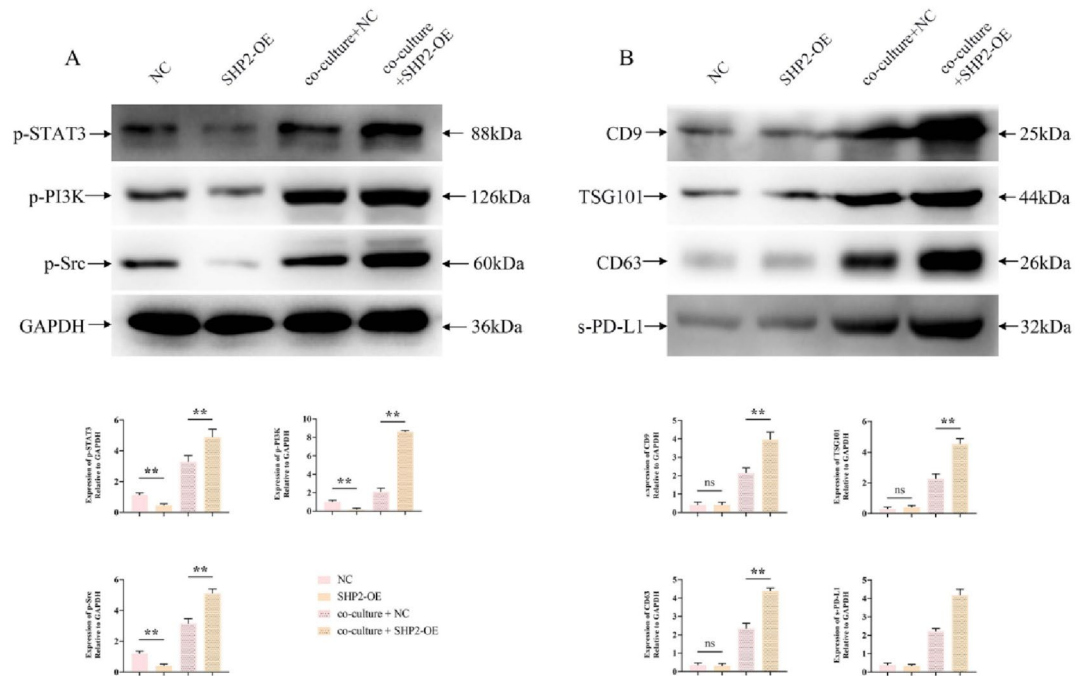


Fig. 4. Effects of SHP2 on the STAT3/PI3K pathway and exosome secretion in CRC TAMs. A: Western blot in THP-1-derived TAMs (all bands from THP-1/TAMs; SW480 was used only to establish co-culture conditions) for p-STAT3, p-PI3K and p-Src. Bar graphs show GAPDH-normalized relative protein levels ($n = 3$, mean \pm SD). B: Western blot of exosomes isolated under the indicated co-culture conditions for CD9, TSG101, CD63 and s-PD-L1. Bar graphs are based on equal protein loading and normalization to CD63/TSG101 ($n = 3$, mean \pm SD). Compared with “co-culture + NC,” the “co-culture + SHP2-OE” group shows significantly increased levels. ns, $P > 0.05$; **, $P < 0.01$.

synergistically in different cell cycle phases to regulate cell proliferation. Cyclin D1 binds to CDK4/6 to form a complex that facilitates the transition of cells from G1 phase to S phase. By initiating the phosphorylation of Rb (retinoblastoma protein), Cyclin D1 releases the E2F transcription factor, which activates the expression of genes in S-phase. Cyclin A binds to CDK2 and regulates DNA replication. In S phase, the Cyclin A/CDK2 complex is responsible for driving DNA synthesis. In G2 phase, it binds to CDK1 and helps prepare the cell for entry into M phase (mitosis). PCNA (Proliferating Cell Nuclear Antigen) is a cofactor for DNA synthesis and acts as a sliding clamp for DNA polymerase, enhancing its efficiency and precision during DNA replication. It plays a key role in S phase to ensure smooth DNA replication. MMP2 and MMP9 are two important members of the family of matrix metalloproteinases (MMPs), which play key roles in cell migration and tissue remodelling. In tumour cells, overexpression of MMP2 is associated with tumour invasion and metastasis. By degrading the basement membrane, MMP2 enables tumour cells to cross the basement membrane and invade blood vessels, leading to distant metastasis. High expression of MMP9 correlates with invasiveness and metastasis. By degrading the extracellular matrix, MMP9 assists tumour cells in crossing the basement membrane and accessing blood vessels and lymphatic vessels, which leads to metastasis.

In this study, the relative protein expression levels of MMP2, MMP9, Cyclin D1, Cyclin A and PCNA in THP-1 cells and the expression levels of CD9, TSG101, CD63, and s-PD-L1 in exosomes of the SHP2-OE group were not significantly different from those of the NC group, while the expression levels of p-STAT3, p-PI3K and p-Src expression levels were slightly decreased in THP-1 cells. After co-culture of THP-1 cells and SW480 cells, the relative protein expression of p-STAT3, p-PI3K, p-Src, MMP2, MMP9, Cyclin D1, Cyclin A and PCNA in THP-1 cells in the SHP2-OE group and the relative protein expression of CD9, TSG101, CD63, CD63, and s-PD-L1 in exosomes were not significantly different from the NC group, as compared with the NC group, and s-PD-L1 expression levels were significantly increased^{17,24}. In addition, after co-culture of THP-1 cells with SW480 cells, SHP2 overexpression could promote the proliferation, migration and invasion ability of SW480 cells.

CAR-T cell (chimeric antigen receptor T cell) therapy is an immunotherapy technique that has been shown to be effective in haematological malignancies such as acute lymphoblastic leukaemia and multiple myeloma. CAR-T cell therapy works by extracting T cells from the patient's body and genetically engineering them to become specific T cells that can recognise and attack cancer cells. The modified T-cells carry chimeric antigen receptors (CARs) that recognise specific antigens on the surface of cancer cells, activate the T-cells and kill the cancer cells. However, the tumour microenvironment of colorectal cancer is very complex, with the presence of a large number of immunosuppressive factors that can inhibit the activity of CAR-T cells. The PD-1 (programmed death receptor-1) and PD-L1 (programmed death ligand-1) pathways are a key immunosuppressive mechanism utilised by tumour cells. PD-1 is an inhibitory receptor that is predominantly expressed on the surfaces of

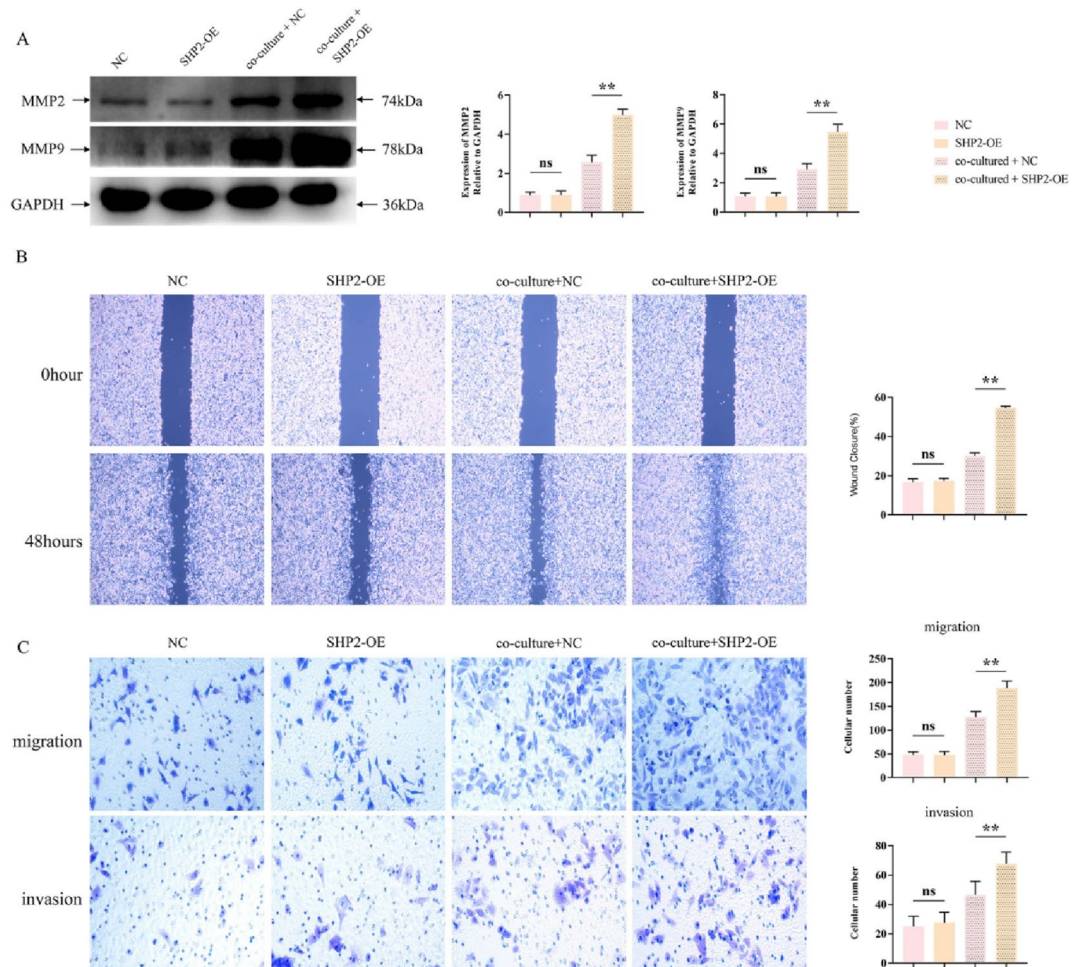


Fig. 5. Effects of SHP2 on the migration and invasion of CRC cells. **A:** Western blot in THP-1/TAMs (all bands from THP-1/TAMs) for MMP-2 and MMP-9; bar graphs show GAPDH-normalized relative expression ($n = 3$, mean \pm SD). **B:** Images acquired with a $10\times$ objective under identical exposure/gain; scale bar, $200\ \mu\text{m}$. Scratches made with a $200\text{-}\mu\text{L}$ tip (minor initial-width variation); wound closure normalized to each well's 0-h width. $n = 3$ biological replicates per group; ≥ 5 fields per replicate; technical replicates averaged before statistics. **C:** SW480 Transwell migration/invasion assays and cell counts. SHP2 overexpression in TAMs increases MMPs in TAMs and promotes SW480 migration and invasion. ns, $P > 0.05$; **, $P < 0.01$.

activated T-cells, B-cells and some immune cells. PD-L1, a ligand for PD-1, is widely expressed on tumour cells, tumour-associated immune cells (e.g. macrophages) and normal tissue cells. When PD-1 binds to PD-L1, it is able to transmit inhibitory signals to T cells, leading to T cell failure, reduced proliferation and cytotoxicity, thus allowing tumour cells to evade immune surveillance^{25–27}. In the above study, we found that SHP2 overexpression in TAMs could mediate the STAT3/PI3K signalling pathway to promote exosome secretion as well as s-PD-L1 expression. Bax (Bcl-2-associated X protein) is a pro-apoptotic protein belonging to the Bcl-2 family. Activation of Bax forms pores in the outer mitochondrial membrane, leading to an increase in the permeability of the outer mitochondrial membrane, which results in the release of cytochrome C and other pro-apoptotic factors (e.g. SMAC/DIABLO) from the mitochondria into the cytoplasm. And cytochrome C release can activate the downstream caspase cascade reaction, which triggers apoptosis. Activated Caspase-9 initiates the execution phase of apoptosis by cleaving and activating execution-type caspases such as Caspase-3, which is the main executing enzyme of apoptosis and is known as the 'apoptosis executor' and plays a central role in the final phase of apoptosis. It cleaves and activates Caspase-activated DNase (CAD), which leads to the ordered fragmentation of DNA, one of the typical hallmarks of apoptosis. And in our subsequent study, in CAR-T cells, there was no significant difference in the relative protein expression of Bax, Caspase-3 and Caspase-9 in the SHP2-OE group relative to the NC group. After co-culture of SW480 cells with THP-1 cells and CAR-T cells, the relative protein expression of Bax, Caspase-3 and Caspase-9 were significantly increased in the SHP2-OE group compared with the NC group. After the addition of PD-1 monoclonal antibody, the above indexes were significantly reduced and the significant difference was eliminated in both groups.

Limitations and future directions. This study is primarily based on in vitro correlative evidence and lacks validation across multiple models, genetic loss-of-function/rescue, and in vivo experiments. Going forward,

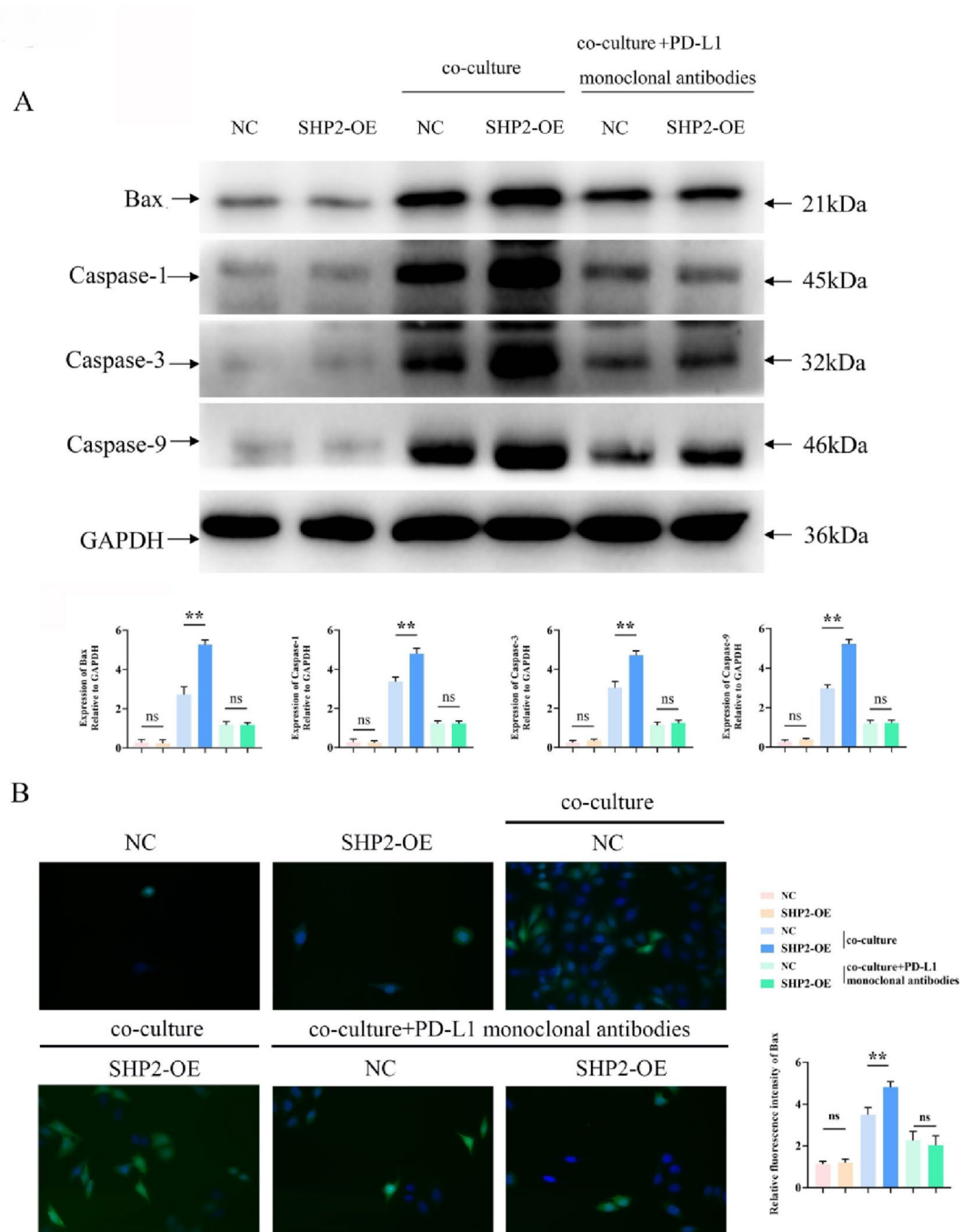


Fig. 6. Effects of SHP2 on CAR-T cell apoptosis in the CRC microenvironment. **A:** Western blot in CAR-T cells (all bands from CAR-T cells) for Bax, Caspase-1, Caspase-3 and Caspase-9; bar graphs show GAPDH-normalized relative protein levels ($n = 3$, mean \pm SD), under co-culture \pm anti-PD-L1 monoclonal antibody. **B:** Green indicates Bax immunofluorescence (Alexa Fluor 488) and blue indicates DAPI nuclear staining. Images were acquired under identical exposure/gain settings and displayed at the best-focus plane; merged images are shown with a 50 μm scale bar. SHP2 overexpression in TAMs promotes CAR-T apoptosis, which is partially reversed by PD-L1 blockade. ns, $P > 0.05$; **, $P < 0.01$.

we will: (i) replicate key findings across additional CRC cell lines and primary systems; (ii) implement loss-of-function and rescue of SHP2/STAT3/PI3K in TAMs and cross-validate with pharmacologic inhibition; (iii) define the necessity of exosomes by perturbing their biogenesis/uptake and blocking effects on recipient cells; and (iv) conduct TAM-targeted in vivo studies and evaluate combinations with PD-1/PD-L1 blockade or SHP2 inhibitors. These efforts will further establish causality and clarify the translational potential of this axis.

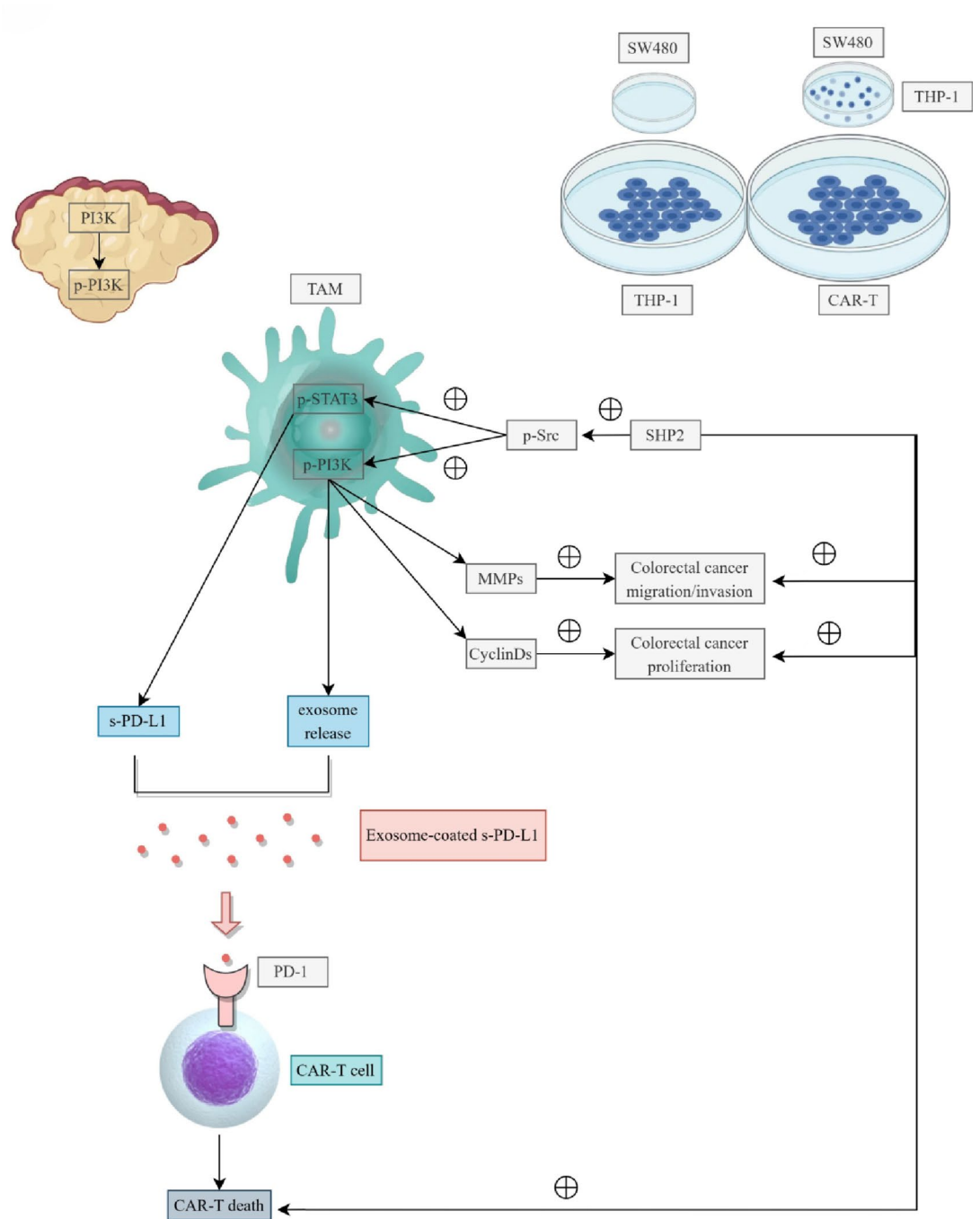


Fig. 7. SHP2 in tumour-associated macrophages promotes colorectal cancer progression by regulating the STAT3/PI3K signalling pathway to induce PD-1-mediated apoptosis of CAR-T cells.

Conclusion

Given the above, activation of TAM-intrinsic SHP2 is significantly associated with upregulation of STAT3/PI3K signaling and PD-1-related CAR-T cell apoptosis, suggesting that it participates in shaping the immunosuppressive microenvironment of CRC and promoting disease progression. This study provides strong rationale for leveraging macrophage SHP2 as an entry point to optimize immunotherapy.

Data availability

The datasets generated during and/or analysed during the current study are available from the corresponding author on reasonable request.

Received: 4 December 2024; Accepted: 10 November 2025

Published online: 29 December 2025

References

- Sung, H. et al. Global cancer statistics 2020: GLOBOCAN estimates of incidence and mortality worldwide for 36 cancers in 185 countries. *CA Cancer J. Clin.* **71**, 209–249 (2021).
- Bastid, C. et al. [Colorectal cancer: technological revolution]. *Rev. Med. Suisse.* **19**, 938–943 (2023).
- Du, B. et al. CAR-T therapy in solid tumors. *Cancer Cell.* **43**, 665–679 (2025).
- Han, B. et al. Cancer incidence and mortality in China, 2022. *J. Natl. Cancer Cent.* **4**, 47–53 (2024).
- Ghazi, B., El Ghanmi, A., Kandoussi, S., Ghoulzani, A. & Badou A. CAR T-cells for colorectal cancer immunotherapy: ready to go. *Front. Immunol.* **13**, 978195 (2022).
- Qin, X., Wu, F., Chen, C. & Li, Q. Recent advances in CAR-T cells therapy for colorectal cancer. *Front. Immunol.* **13**, 904137 (2022).
- Li, H., Yang, C., Cheng, H., Huang, S. & Zheng, Y. CAR-T cells for colorectal cancer: Target-selection and strategies for improved activity and safety. *J. Cancer.* **12**, 1804–1814 (2021).
- Zheng, Z. et al. Cells in Colorectal Cancer: Unravelling the Function of Different T Cell Subsets in the Tumor Microenvironment. *Int J. Mol. Sci.* **24** (2023).
- Chai, G., Nan, Y., Zhao, H. & Hu, Q. SHP2 mediates STAT3/STAT6 signaling pathway in TAM to inhibit proliferation and metastasis of lung adenocarcinoma. *Aging (Albany NY).* **16**, 12498–12509 (2024).
- Wei, Q., Luo, S. & He, G. Mechanism study of tyrosine phosphatase shp-1 in inhibiting hepatocellular carcinoma progression by regulating the SHP2/GM-CSF pathway in TAMs. *Sci. Rep.* **14**, 9128 (2024).
- Gao, J. et al. Allosteric Inhibition reveals SHP2-mediated tumor immunosuppression in colon cancer by single-cell transcriptomics. *Acta Pharm. Sin B.* **12**, 149–166 (2022).
- Kanehisa, M., Sato, Y., Kawashima, M., Furumichi, M. & Tanabe, M. KEGG as a reference resource for gene and protein annotation. *Nucleic Acids Res.* **44**, D457–462 (2016).
- Kanehisa, M. & Goto, S. KEGG: Kyoto encyclopedia of genes and genomes. *Nucleic Acids Res.* **28**, 27–30 (2000).
- Li, J., Ma, X., Chakravarti, D., Shalapour, S. & DePinho, R. A. Genetic and biological hallmarks of colorectal cancer. *Genes Dev.* **35**, 787–820 (2021).
- Li, Q. et al. Signaling pathways involved in colorectal cancer: pathogenesis and targeted therapy. *Signal. Transduct. Target. Ther.* **9**, 266 (2024).
- Vaziri-Moghadam, A. & Foroughmand-Araabi, M. H. Integrating machine learning and bioinformatics approaches for identifying novel diagnostic gene biomarkers in colorectal cancer. *Sci. Rep.* **14**, 24786 (2024).
- Welsh, J. A. et al. Minimal information for studies of extracellular vesicles (MISEV2023): from basic to advanced approaches. *J. Extracell. Vesicles.* **13**, e12404 (2024).
- Yue, Y., Zhang, Q. & Sun, Z. CX3CR1 acts as a protective biomarker in the tumor microenvironment of colorectal cancer. *Front. Immunol.* **12**, 758040 (2021).
- Wang, X. et al. HMG2 facilitates colorectal cancer progression via STAT3-mediated tumor-associated macrophage recruitment. *Theranostics* **12**, 963–975 (2022).
- Zhu, G. et al. Phase separation of Disease-Associated SHP2 mutants underlies MAPK hyperactivation. *Cell* **183**, 490–502e18 (2020).
- Sun, Z. et al. Targeting macrophagic SHP2 for ameliorating osteoarthritis via TLR signaling. *Acta Pharm. Sin B.* **12**, 3073–3084 (2022).
- Heynen, G. et al. Targeting SHP2 phosphatase in breast cancer overcomes RTK-mediated resistance to PI3K inhibitors. *Breast Cancer Res.* **24**, 23 (2022).
- Song, Z. et al. Tyrosine phosphatase SHP2 inhibitors in tumor-targeted therapies. *Acta Pharm. Sin B.* **11**, 13–29 (2021).
- Zhou, K., Guo, S., Li, F., Sun, Q. & Liang, G. Exosomal PD-L1: new insights into tumor immune escape mechanisms and therapeutic strategies. *Front. Cell. Dev. Biol.* **8**, 569219 (2020).
- Ray, S. K., Meshram, Y. & Mukherjee, S. Cancer immunology and CAR-T cells: A turning point therapeutic approach in colorectal carcinoma with clinical insight. *Curr. Mol. Med.* **21**, 221–236 (2021).
- He, S. et al. CD166-specific CAR-T cells potently target colorectal cancer cells. *Transl Oncol.* **27**, 101575 (2023).
- Jin, K. T., Chen, B., Liu, Y. Y., Lan, H. U. & Yan, J. P. Monoclonal antibodies and chimeric antigen receptor (CAR) T cells in the treatment of colorectal cancer. *Cancer Cell. Int.* **21**, 83 (2021).

Author contributions

G.Y. W and J.F. X responsible for the drafting of manuscripts and the collection and analysis of data. X.Y. Z and J.B.C were responsible for cell culture and migration assays. Z.B. Z Conceptualized the study, performed the literature review, All authors participated in the revision of the manuscript.

Funding

None.

Declarations

Competing interests

The authors declare no competing interests.

Additional information

Supplementary Information The online version contains supplementary material available at <https://doi.org/10.1038/s41598-025-28261-6>.

Correspondence and requests for materials should be addressed to G.W.

Reprints and permissions information is available at www.nature.com/reprints.

Publisher's note Springer Nature remains neutral with regard to jurisdictional claims in published maps and institutional affiliations.

Open Access This article is licensed under a Creative Commons Attribution-NonCommercial-NoDerivatives 4.0 International License, which permits any non-commercial use, sharing, distribution and reproduction in any medium or format, as long as you give appropriate credit to the original author(s) and the source, provide a link to the Creative Commons licence, and indicate if you modified the licensed material. You do not have permission under this licence to share adapted material derived from this article or parts of it. The images or other third party material in this article are included in the article's Creative Commons licence, unless indicated otherwise in a credit line to the material. If material is not included in the article's Creative Commons licence and your intended use is not permitted by statutory regulation or exceeds the permitted use, you will need to obtain permission directly from the copyright holder. To view a copy of this licence, visit <http://creativecommons.org/licenses/by-nc-nd/4.0/>.

© The Author(s) 2025